ChemComm

COMMUNICATION

View Article Online
View Journal | View Issue

Cite this: *Chem. Commun.*, 2016, 52, 10008

Received 27th April 2016,
Accepted 14th July 2016

DOI: 10.1039/c6cc03536a

www.rsc.org/chemcomm

Extended conjugated microporous polymers for photocatalytic hydrogen evolution from water†

Reiner Sebastian Sprick,[a] Baltasar Bonillo,[a] Michael Sachs,[b] Rob Clowes,[a] James R. Durrant,[b] Dave J. Adams[a] and Andrew I. Cooper*[a]

Conjugated microporous polymers (CMPs) have been used as photocatalysts for hydrogen production from water in the presence of a sacrificial electron donor. The relative importance of the linker geometry, the co-monomer linker length, and the degree of planarisation were studied with respect to the photocatalytic hydrogen evolution rate.

Conjugated microporous polymers (CMPs) have been studied for applications such as gas storage,[1,2] separations,[3] energy storage,[4] and catalysis.[5,6] CMPs have also been used as photocatalysts for light-driven dye-degradation,[7,8] oxidation of natural products,[9] and coupling reactions.[10,11] A more recent development has been their use as photocatalysts for hydrogen evolution.[12] Most water splitting photocatalysts are either inorganic solids,[13,14] graphitic carbon nitrides (g-C_3N_4),[15–18] or other related structures,[19–22] such as triazine networks.[23] Far fewer organic materials have been studied for this application,[24,25] even though the scope for structural diversity[26] and high-yielding syntheses[27] (*e.g.*, compared to g-C_3N_4)[18] suggest potential advantages. We showed that CMPs evolve hydrogen from water under visible light in the presence of a sacrificial donor.[12,28] Subsequently, we showed that rigid, linear fluorene-type phenylene co-polymers are even more active as photocatalysts.[19] Unlike our earlier CMPs,[12] these fluorene materials are non-porous due to their efficient π–π packing in the solid-state.[19]

While the potential for CMPs as photocatalysts for hydrogen evolution has been demonstrated, the associated design rules are not well understood. Hence, there is a need to investigate the catalytic efficiency of different CMPs such that more detailed structure–property relationships can be established. Here, we study the influence of substitution patterns and conjugation length on the photocatalytic performance for a series of CMP materials.

We have previously reported band gap tuning *via* statistical co-polymerisation of monomers to create CP-CMP materials[12] and also the doping of CP-CMPs with small molar quantities of co-monomers to tune the optical properties.[29] In this new study, we explore the effect of changing the monomer linker length and type of linkage and the resulting performance in photocatalytic hydrogen production from water.

In addition to the previously reported CP-CMP1,[12] we prepared an extended biphenyl analogue (PE-CMP, Fig. 1). Poly(*meta*-phenylene)s have been reported to have wide band-gaps,[30] and we therefore synthesised a 1,3,5-linked analogue (M-CMP), and its extended analogue (ME-CMP).[31] Finally, we applied the concept of planarisation[19] and synthesised a spirobifluorene CMP (SP-CMP) and its extended analogue (ESP-CMP).[27] In all cases, the polymerisations were carried out using Pd(0)-catalysed Suzuki–Miyaura polycondensation at 150 °C for 2 days before work-up and Soxhlet extraction to remove low-molecular weight by-products (see ESI† for full details).

All materials were recovered as insoluble solids and characterised by elemental analysis, Fourier-transform infrared

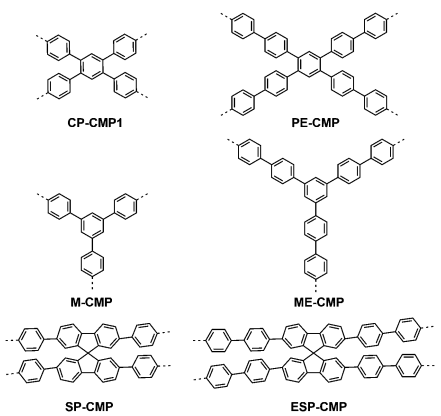

Fig. 1 Structures of the conjugated microporous polymers.[32]

[a] *Department of Chemistry and Centre for Materials Discovery, University of Liverpool, Crown Street, Liverpool, L69 7ZD, UK. E-mail: aicooper@liverpool.ac.uk*
[b] *Department of Chemistry, Imperial College London, South Kensington Campus, London SW7 2AZ, UK*

† Electronic supplementary information (ESI) available: Full experimental details, gas sorption isotherms, UV-vis, PL, and FT-IR spectra, PXRD, SEM, hydrogen evolution experiments, suspension PL spectra, and TCSPC experiments. See DOI: 10.1039/c6cc03536a

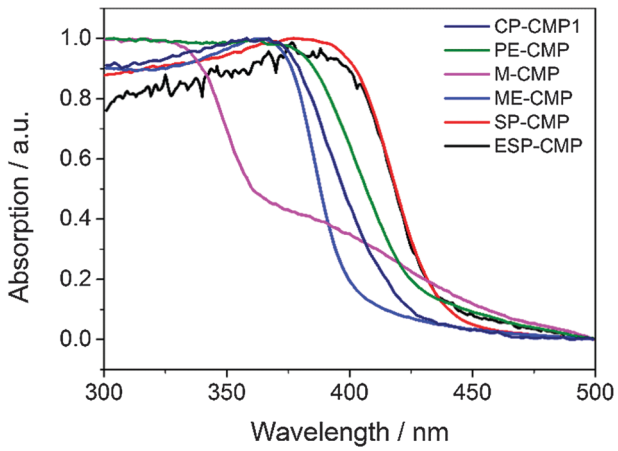

Fig. 2 UV/vis reflectance spectra of the CMPs in the solid-state.

spectroscopy (FT-IR), thermogravimetric analysis (TGA), scanning electron microscope (SEM), energy-dispersive X-ray spectroscopy (EDX), and powder X-ray diffraction (PXRD). TGA showed that the CMPs were stable up to 300 °C under air and SEM revealed particles ranging from 100 to 250 nm and all materials had broadly similar particle size ranges, but the morphologies varied. CP-CMP1 and SP-CMP consisted of spherical particles, ME-CMP, PE-CMP and ESP-CMP formed flake-like particles, and M-CMP formed elongated, fused spherical particles. All CMPs have bromine, present most likely as end-groups, as shown by EDX (0.23 to 0.96 wt%). PXRD patterns showed that all materials were amorphous. CP-CMP1, PE-CMP, M-CMP and SP-CMP were porous to nitrogen at 77 K, with apparent Brunauer–Emmett–Teller surface areas (SA_{BET}) between 489 and 895 $m^2\ g^{-1}$; SP-CMP was the most porous polymer in this study. By contrast, ME-CMP did not show significant uptake of nitrogen at 77 K, but it was porous to hydrogen at this temperature (see ESI†). A red-shift of the absorption on-set in the solid-state UV-visible reflectance spectra was observed when extending the phenyl-linker in CP-CMP1 to biphenyl in PE-CMP (Fig. 2). The 1,3,5-linked M-CMP showed a two-stage absorption profile, which was also observed previously for other CMPs,[10] with a broad absorption around 400 nm and a sharp on-set at 340 nm. As for the CP-CMP1 and PE-CMP polymers, extension to biphenyl results in a red shift of the on-set for ME-CMP. However, both M-CMP and ME-CMP are blue shifted relative to their 1,2,4,5-linked analogues (CP-CMP1 and PE-CMP), both in their absorption on-sets, and also in their photoluminescence maxima (see ESI†). These observations agree with computational predictions for oligo(phenylene)s[33] and indicate a lower effective conjugation length for the *meta*-linked CMPs. The spirobifluorene-linked CMPs (SP-CMP and ESP-CMP) are both red-shifted with respect to PE-CMP, both for the absorption on-set and the photoluminescence maximum, indicating a greater effective conjugation length.

All materials were tested for their performance as photocatalysts for hydrogen evolution from water. In contrast to our previous report,[12] we used triethylamine (TEA) as sacrificial electron donor instead of diethylamine. We found that mixtures of triethylamine and methanol led to significantly increased hydrogen evolution rates. Methanol does not act as a sacrificial donor, but seems to act as a co-solvent, thus avoiding phase separation between water and the TEA;[19] a similar effect was found when acetonitrile was used instead of methanol (see ESI†). All CMPs were used as-synthesised, after purification, and no additional metal co-catalysts (*e.g.*, Pt) were added. However, significant levels of palladium (0.3–0.9 wt%) were found in all materials by ICP-OES (see ESI†), and palladium is known to act as a co-catalyst for g-C_3N_4.[34] Hence, as for our previous CP-CMP study,[12] it is not possible to eliminate the possible role of Pd residues in the catalytic mechanism, although carbon monoxide poisoning experiments in our earlier study had no effect on the hydrogen evolution rate.

Most of these CMPs materials could act as photocatalysts for hydrogen evolution, although to greatly varying degrees (Fig. 3). No hydrogen was evolved from the water/sacrificial donor mixtures under either >295 nm or >420 nm illumination in the absence of the CMPs. The efficiency of the CMPs as photocatalysts was strongly related to their chemical structure. PE-CMP showed higher hydrogen evolution rates than CP-CMP1, both under combined UV/visible light (17.9 μmol h^{-1} *vs.* 4.1 μmol h^{-1}, >295 nm) and under visible light (0.5 μmol h^{-1} *vs.* 0.2 μmol h^{-1}; >420 nm), although the activity of both materials was rather low.

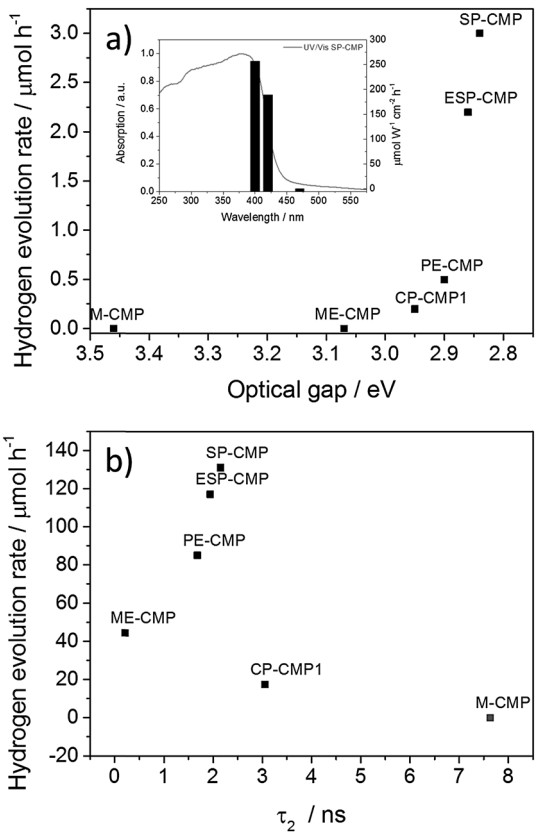

Fig. 3 (a) Hydrogen evolution rates under visible light (λ > 420 nm) correlated with the optical gap of the CMPs. Each measurement was performed with 25 mg catalyst in water/MeOH/triethylamine mixture. Wavelength dependency of the photocatalytic hydrogen evolution for SP-CMP (insert). (b) Correlation of the life-time of the excited state with hydrogen evolution rates under broadband illumination (λ > 295 nm).

The incorporation of the 1,3,5-linker into M-CMP resulted in the complete loss of activity under visible illumination (>420 nm or >400 nm). Under >295 nm illumination, only a very small amount of hydrogen was evolved. Extension of the structure from phenyl to biphenyl (ME-CMP) resulted in significant increase of activity under combined UV and visible light (9.8 μmol h^{-1}; >295 nm) compared to M-CMP, outperforming CP-CMP1 under these conditions. By contrast, the activity is observed under >400 nm incident light was low, and no activity at all was observed under >420 nm illumination. *meta*-Linkages in CMPs have been reported before to reduce the effective π-conjugation length,[35] and the lack of light absorption that this causes explains these trends (Fig. 1). Furthermore, *meta*-linkages in linear conjugated polymers have been shown to be detrimental to achieving high molecular weights,[36] and this might also impact the photocatalytic performance. When spirobifluorene was incorporated, the photocatalytic activity was significantly enhanced. SP-CMP showed the highest higher hydrogen evolution rate under broadband illumination (28.8 μmol h^{-1}, >295 nm) and a hydrogen evolution rate under visible light (3.0 μmol h^{-1}; >420 nm) that was 15 times higher than CP-CMP1. Further extension of the linkers in SP-CMP by incorporating biphenyl (ESP-CMP) did not significantly change the photocatalytic activity, and a similar absorption on-set was observed (Table 1). An apparent quantum yield of 0.23% at 420 nm (±10 nm fwhm) was determined for SP-CMP, which is higher than for linear, non-porous poly(*p*-phenylene) ($AQY_{420\,nm}$ = 0.1%) or platinised commercial graphitic carbon nitride ($AQY_{420\,nm}$ = 0.1%).[19]

The photostability of SP-CMP was evaluated by running a sample for 74 hours under >420 nm illumination, followed by 44 hours under >295 nm illumination (Fig. 4). The CMP powder was recovered by filtration and dried. Analysis *via* N_2 sorption, FT-IR, UV/vis and PL showed no significant changes to the material properties, both suggesting good stability and also ruling out the polymer as the source of hydrogen.

The life-time of the excited state was estimated by time-correlated single photon counting for the CMP powders suspended in THF (Table 2). Extension of the struts from phenyl to biphenyl reduced lifetimes, both for PE-CMP (τ_1 = 0.42 ns, τ_2 = 1.68 ns)/CP-CMP1 (τ_1 = 0.76 ns, τ_2 = 3.05 ns), and for ME-CMP (τ_1 = 0.05 ns, τ_2 = 0.21 ns)/M-CMP (τ_1 = 1.91 ns, τ_2 = 7.63 ns). By contrast, in the case of SP-CMP (τ_1 = 0.54 ns, τ_2 = 2.15 ns) and ESP-CMPs (τ_1 = 0.49 ns, τ_2 = 1.94 ns), little difference was observed when the linker length was increased.

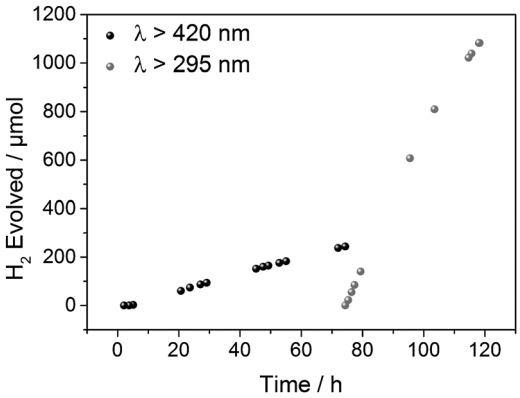

Fig. 4 Hydrogen experiment of SP-CMP under visible light (λ > 420 nm) for 74 hours followed by a further 44 hours under combined UV and visible light (λ > 295 nm). The experiment was performed with 25 mg catalyst in water/MeOH/triethylamine mixture.

This possibly indicates that life-time of the excited state is not the primary, limiting factor for the photocatalytic performance of these materials, but that this is dominated instead by the gain in light absorption upon increasing the linker length, which outweighs the reduced excited state lifetime. Since M-CMP does not evolve hydrogen from water, the TCSPC result is therefore ambiguous and we also noticed that the fluorescence intensity of CP-CMP1 and M-CMP are lower in the TCSPC measurements. However, when comparing the lifetimes of the series ME-CMP, PE-CMP, ESP-CMP, and SP-CMP, then longer lifetimes of the excited state do seem to correlate, broadly, with the observed photocatalytic performance (Fig. 3b).

While none of these polymers is highly active under visible light (λ > 420 nm) compared to materials in our previous report,[19] due to a lack of visible light absorption, the increase in activity observed under UV light (λ > 295 nm) with respect to CP-CMP1 is significant and shows that extended linkers and fused, planar monomers lead to increased photocatalytic activity.

SP-CMP shows both the highest porosity and the highest photocatalytic performance, but no general correlation between surface area and photocatalytic performance was found. Rather, there is a strong correlation between photocatalytic performance and their light absorption profiles, and 1,3,5-linkages are strongly detrimental to the photocatalytic performance because the absorption on-sets are significantly blue-shifted. PL lifetime is only partially correlated with activity (Fig. 3b), since other factors,

Table 1 Surface areas, optical properties and photocatalytic performance of the CMPs

	SA_{BET}[a]/$m^2\ g^{-1}$	E_g^{OPT}[b]/eV	HER[c] >420 nm/μmol h^{-1}	HER[c] >400 nm/μmol h^{-1}	HER[c] >295 nm/μmol h^{-1}
CP-CMP1	683	2.95	0.2	1.4	4.1
PE-CMP	489	2.90	0.5	2.5	17.9
M-CMP	570	3.46	0	0	<0.1
ME-CMP	41	3.07	0	0.2	9.8
SP-CMP	895	2.84	3.0	8.0	28.8
ESP-CMP	522	2.86	2.2	9.8	28.2

[a] Apparent BET surface area, SA_{BET}, as calculated from the N_2 adsorption isotherm. [b] Calculated from the onset of the absorption spectrum in the solid-state. [c] Hydrogen evolution rates (HER) determined with 25 mg catalyst in water/MeOH/triethylamine mixture irradiated by 300 W Xe lamp for 5 hours using a suitable filter.

Table 2 Time-correlated single-photon counting results for the CMPs

	Fitted decay time τ_1[a]/ns	Fitted decay time τ_2[a]/ns
CP-CMP1	0.76	3.05
PE-CMP	0.42	1.68
M-CMP	1.91	7.63
ME-CMP	0.05	0.21
SP-CMP	0.54	2.15
ESP-CMP	0.49	1.94

[a] Calculated by fitting the following equation: $A + B1 \times \exp(-i/\tau_1) + B2 \times \exp(-i/\tau_2)$. Initial amplitudes ($A$, $B1$, $B2$) are estimated and iterated along with the lifetimes (τ_1, τ_2) until a fit is found. The prompt is measured separately and used for deconvolution of the instrument response.

such as the lack of light absorption, can become dominant. The two best-performing materials in this study, SP-CMP and ESP-CMP, combine high surface areas and photocatalytic activities that are greatly improved over linear, not porous poly(*p*-phenylene).[19,25] This combination of properties might also be useful for other applications, such as photocatalytic organic reactions.

We thank the Engineering and Physical Sciences Research Council (EPSRC) for financial support under Grant EP/N004884/1. MS and JRD acknowledge support of ERC AdG Intersolar (291482) and Imperial College PhD Scholarship. DA thanks the EPSRC for a Fellowship (EP/L021978/1). The authors would like to thank M. Zwijnenburg for helpful discussions.

Notes and references

1 Y. Xu, S. Jin, H. Xu, A. Nagai and D. Jiang, *Chem. Soc. Rev.*, 2013, **42**, 8012–8031.
2 A. I. Cooper, *Adv. Mater.*, 2009, **21**, 1291–1295.
3 A. Li, H.-X. Sun, D.-Z. Tan, W.-J. Fan, S.-H. Wen, X.-J. Qing, G.-X. Li, S.-Y. Li and W.-Q. Deng, *Energy Environ. Sci.*, 2011, **4**, 2062.
4 Y. Kou, Y. Xu, Z. Guo and D. Jiang, *Angew. Chem., Int. Ed.*, 2011, **50**, 8753–8757.
5 J.-X. Jiang, C. Wang, A. Laybourn, T. Hasell, R. Clowes, Y. Z. Khimyak, J. Xiao, S. J. Higgins, D. J. Adams and A. I. Cooper, *Angew. Chem.*, 2011, **123**, 1104–1107.
6 Y. Xie, T.-T. Wang, X.-H. Liu, K. Zou and W.-Q. Deng, *Nat. Commun.*, 2013, **4**, 1960.
7 B. C. Ma, S. Ghasimi, K. Landfester, F. Vilela and K. A. I. Zhang, *J. Mater. Chem. A*, 2015, **3**, 16064–16071.
8 S. Ghasimi, S. Prescher, Z. J. Wang, K. Landfester, J. Yuan and K. A. I. Zhang, *Angew. Chem., Int. Ed.*, 2015, **54**, 14549–14553.
9 K. Zhang, D. Kopetzki, P. H. Seeberger, M. Antonietti and F. Vilela, *Angew. Chem., Int. Ed.*, 2013, **52**, 1432–1436.
10 Z. J. Wang, S. Ghasimi, K. Landfester and K. A. I. Zhang, *Adv. Mater.*, 2015, **27**, 6265–6270.
11 J. X. Jiang, Y. Li, X. Wu, J. Xiao, D. J. Adams and A. I. Cooper, *Macromolecules*, 2013, **46**, 8779–8783.
12 R. S. Sprick, J. Jiang, B. Bonillo, S. Ren, T. Ratvijitvech, P. Guiglion, M. A. Zwijnenburg, D. J. Adams and A. I. Cooper, *J. Am. Chem. Soc.*, 2015, **137**, 3265–3270.
13 D. M. Fabian, S. Hu, N. Singh, F. A. Houle, T. Hisatomi, K. Domen, F. Osterloh and S. Ardo, *Energy Environ. Sci.*, 2015, **8**, 2825–2850.
14 A. Kudo and Y. Miseki, *Chem. Soc. Rev.*, 2009, **38**, 253–278.
15 X. Wang, K. Maeda, A. Thomas, K. Takanabe, G. Xin, J. M. Carlsson, K. Domen and M. Antonietti, *Nat. Mater.*, 2009, **8**, 76–80.
16 X. Wang, S. Blechert and M. Antonietti, *ACS Catal.*, 2012, **2**, 1596–1606.
17 S. Cao and J. Yu, *J. Phys. Chem. Lett.*, 2014, **5**, 2101–2107.
18 J. Liu, Y. Liu, N. Liu, Y. Han, X. Zhang, H. Huang, Y. Lifshitz, S.-T. Lee, J. Zhong and Z. Kang, *Science*, 2015, **347**, 970–974.
19 R. S. Sprick, B. Bonillo, R. Clowes, P. Guiglion, N. J. Brownbill, B. J. Slater, F. Blanc, M. A. Zwijnenburg, D. J. Adams and A. I. Cooper, *Angew. Chem., Int. Ed.*, 2016, **55**, 1792–1796.
20 K. Schwinghammer, S. Hug, M. B. Mesch, J. Senker and B. V. Lotsch, *Energy Environ. Sci.*, 2015, **8**, 3345–3353.
21 V. S. Vyas, F. Haase, L. Stegbauer, G. Savasci, F. Podjaski, C. Ochsenfeld and B. V. Lotsch, *Nat. Commun.*, 2015, **6**, 8508.
22 K. Kailasam, J. Schmidt, H. Bildirir, G. Zhang, S. Blechert, X. Wang and A. Thomas, *Macromol. Rapid Commun.*, 2013, **34**, 1008–1013.
23 J. Bi, W. Fang, L. Li, J. Wang, S. Liang, Y. He, M. Liu and L. Wu, *Macromol. Rapid Commun.*, 2015, **36**, 1799–1805.
24 M. G. Schwab, M. Hamburger, X. Feng, J. Shu, H. W. Spiess, X. Wang, M. Antonietti and K. Müllen, *Chem. Commun.*, 2010, **46**, 8932–8934.
25 S. Yanagida, A. Kabumoto, K. Mizumoto, C. Pac and K. Yoshino, *J. Chem. Soc., Chem. Commun.*, 1985, 474.
26 J.-S. Wu, S.-W. Cheng, Y.-J. Cheng and C.-S. Hsu, *Chem. Soc. Rev.*, 2015, **44**, 1113–1154.
27 J. Weber and A. Thomas, *J. Am. Chem. Soc.*, 2008, **130**, 6334–6335.
28 V. S. Vyas and B. V. Lotsch, *Nature*, 2015, **521**, 41–42.
29 B. Bonillo, R. S. Sprick and A. I. Cooper, *Chem. Mater.*, 2016, **28**, 3469–3480.
30 Y. Kan, Y. Zhu, Z. Liu, L. Zhang, J. Chen and Y. Cao, *Macromol. Rapid Commun.*, 2015, **36**, 1393–1401.
31 K. V. Rao, S. Mohapatra, C. Kulkarni, T. K. Maji and S. J. George, *J. Mater. Chem.*, 2011, **21**, 12958.
32 Due to the presence of end-groups and defects in the CMPs the actual structure is far more complex than shown in this simple schematic representation.
33 P. Guiglion and M. Zwijnenburg, *Phys. Chem. Chem. Phys.*, 2015, **17**, 17854–17863.
34 Y. Wang, X. Wang and M. Antonietti, *Angew. Chem., Int. Ed.*, 2012, **51**, 68–89.
35 Y. Xu and D. Jiang, *Chem. Commun.*, 2014, **50**, 2781.
36 J. Ritchie, J. a. Crayston, J. P. J. Markham and I. D. W. Samuel, *J. Mater. Chem.*, 2006, **16**, 1651.